Advances in Computational Engineering & Sciences, Vol. I;
Eds. S. N. Atluri, F. W. Brust; Tech Science Press, Palmdale, CA, 2000; pp. 689-694.

Scaling of the Cathode Region of a Long GTA Welding Arc

P. F. Mendez, M. A. Ramirez, G. Trapaga, T. W. Eagar
Department of Materials Science and Engineering
Massachusetts Institute of Technology
Cambridge, MA 02139

Summary

A new technique of order of magnitude scaling [1] has been applied to the modeling of the cathode region of a long GTA welding arc. The estimations obtained are combined with numerical calculations, thus important features of both techniques are present simultaneously: the accuracy of numerical modeling, and the generality and simplicity of algebraic expressions. Power-law expressions for unknowns such as pressure in the cathode spot and maximum plasma velocity are obtained and are consistent with previous analytical work. The cathode spot is considered axisymmetric and isothermal. Dimensional analysis is used to identify dimensionless groups governing the system, and asymptotic considerations are used to chose the most significant ones.

Introduction

The main goal of this work is to demonstrate the application of the technique of order of magnitude scaling [1] to a complex engineering problem: the welding arc. This technique allows the simultaneous use of dimensional analysis and asymptotic considerations such as dominant balance [2]. Dimensional analysis provides an exact description of the functional dependences in the problem, based on a complete set of dimensionless groups. The asymptotic considerations determine the functional expression of the dimensionless groups, and describes their relative importance. This way dimensionless groups of little influence can be discarded without significant loss in accuracy. The asymptotic considerations also provide a scaling for the problem. The scaling factors and relevant dimensionless groups obtained can be combined with numerical calculations in order to express these results latter in a general, non dimensional form.

Previous attempts have been made to provide general and simple expressions that capture the behavior of the arc [3-6]. The results obtained here are consistent with that work, but this work goes further by determining that in the cathode region the discrepancy between the simple algebraic expressions and exact solutions can be almost completely captured by the Reynolds number and the dimensionless arc length, independently of the thermal properties of the plasma for a range of 200 a to 2000 A in at least argon and air.

Description of the Problem

The focus of this paper is on the cathode region of a long arc. This region, represented in Figure 1 is defined as that contained within R_C in the radial direction and extending for a length of Z_S beyond the cathode boundary layer in the axial direction. A long arc is such that the position of the anode has little effect on the behavior of the cathode region. A convenient way of defining the characteristic length Z_S is $Z_S = V_{ZS} / \max(\partial V_Z / \partial Z)$[1]. The cathode spot radius can be calculated as $R_C = (I/pJ_C)^{1/2}$, where the critical current density J_C depends only on the electrode temperature (for the numerical simulations it was assumed J_C = 6.5 10^7 A/m^2 for a tungsten electrode, and J_C = 4.4 10^7 A/m^2 for a graphite electrode. The thickness of the cathode boundary layer can be estimated as $\hat{d} = 5(mR_e / rV_{RS})$.

[1] For an explanation of the notation see Figure 1 and the last paragraph of this paper.

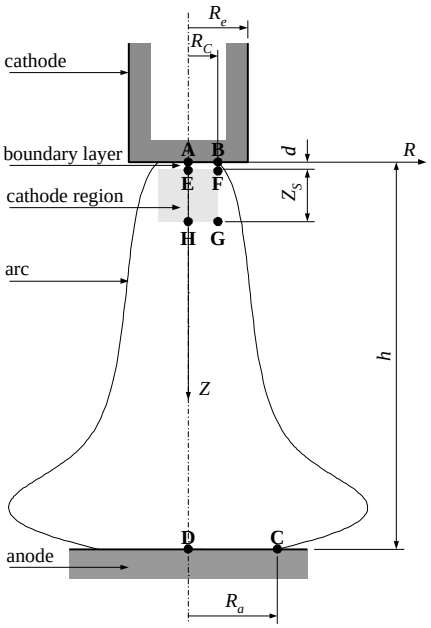

Figure 1
Schematic of a long GTA welding arc , and its cathode region

Experiments [7] and numerical simulations indicate that the temperature variations within the cathode region are small compared to the maximum temperature jump in the arc. This region will be assumed isothermal, with the physical properties corresponding to the maximum temperature in the arc (T_{max}). The governing equations can therefore be simplified as follows:

$$\frac{1}{R}\frac{\partial}{\partial R}(RV_R)+\frac{\partial V_Z}{\partial Z}=0 \tag{1}$$

$$?\left(V_R\frac{\partial V_R}{\partial R}+V_Z\frac{\partial V_R}{\partial Z}\right)=-\frac{\partial P}{\partial R}+m\left[\frac{\partial}{\partial R}\left(\frac{1}{R}\frac{\partial}{\partial R}(RV_R)\right)+\frac{\partial^2 V_R}{\partial Z^2}\right]-J_Z B \tag{2}$$

$$?\left(V_R\frac{\partial V_Z}{\partial R}+V_Z\frac{\partial V_Z}{\partial Z}\right)=-\frac{\partial P}{\partial Z}+m\left[\frac{1}{R}\frac{\partial}{\partial R}\left(R\frac{\partial V_Z}{\partial R}\right)+\frac{\partial^2 V_Z}{\partial Z^2}\right]+J_R B \tag{3}$$

$$m_0 J_R=-\frac{\partial B}{\partial Z} \tag{4}$$

$$m_0 J_Z=\frac{1}{R}\frac{\partial}{\partial R}(RB) \tag{5}$$

$$\frac{\partial^2 B}{\partial Z^2}+\frac{\partial}{\partial R}\left[\frac{1}{R}\frac{\partial}{\partial R}(RB)\right]=0 \tag{6}$$

In the set of equations above, eq. (1) is the equation of conservation of mass, eq. (2) and (3) are the equations of conservation of momentum in R and Z respectively, eq. (4) and (5) represent Ampère's law in R and Z respectively, and eq. (6) is the equation of conservation of magnetic field. In these equations the assumptions are: isothermal (therefore constant density and viscosity), axisymmetric, laminar flow, steady state (this implies a DC arc, or slow current variations), and no magnetic convection (the magnetic Reynolds is very low). The boundary conditions for the scaling of the system are listed in Table 1 and Table 2.

Scaling of the Electromagnetic Field

Because constant properties are used, the governing equations for the electromagnetic field can be decoupled. These equations contain the following complete set of parameters $\{P\}=\{m_0, R_c, J_c, R_a, h\}$, with the following subset of dimensionally independent parameters $\{P_k\}=\{m_0, R_c, J_c\}$, therefore only two dimensionless groups are necessary to describe this system: $\{\Pi\}=\{h/R_C, R_a/R_C\}$. The boundary conditions for the scaling of the electromagnetic field are represented in Table 1. Previous knowledge about the problem (from experiments and numerical models) indicate that the functions vary smoothly between the corner points; this is an important requisite for the application of the order of magnitude scaling technique.

Table 1
Boundary conditions for the scaling of the electromagnetic field

	A	**B**	**C**	**D**
B	0	$\frac{1}{2} m_0 J_C R_C$	$\frac{1}{2} m_0 J_C {R_C}^2 / R_a$	0

The functions describing the electromagnetic field can be scaled with the following relationships:

$$R = R_a r' \tag{7}$$

$$Z = h z' \tag{8}$$

$$J_R(R,Z) = J_{RS}\, j_r(r',z') \tag{9}$$

$$J_Z(R,Z) = J_C\, j_z(r',z') \tag{10}$$

$$B(R,Z) = \tfrac{1}{2} m_0 \frac{{R_C}^2}{R_a} J_C r' \left[1 + \left(\frac{{R_a}^2}{{R_C}^2} - 1 \right) b(r',z') \right] \tag{11}$$

The scaling of $B(R, Z)$ is such that $b(r',z') = 1$ at point **B** in Figure 1, $b(r',z') = 0$ at point **J** in Figure 1, and $B(R, Z)$ increases linearly at R=0, as eq. (4) to (6) indicate. The radius of the anode spot (R_a) depends on the electrical properties of the plasma, which are determined by the heat transfer in the arc. The characteristic value J_{RS} could be estimated by balancing equation (4). Normally for welding arcs, $\Delta R / R_C > 1$, where $\Delta R = R_a - R_C$.

$$\hat{J}_{RS} = \begin{cases} J_C \dfrac{R_c \Delta R}{h R_a} & \text{for } \dfrac{\Delta R}{R_C} < 1 \\ J_C \dfrac{\Delta R^2}{h R_a} & \text{for } \dfrac{\Delta R}{R_C} \geq 1 \end{cases} \tag{12}$$

Scaling of the Fluid Flow

The equations governing the coupled electromagnetic field and fluid flow in the cathode region (eq. (1) to (6)) contain the following complete set of parameters $\{P\}=\{r, m, m_0, R_c, J_c, R_a, h, R_e\}$, with the following subset of dimensionally independent parameters $\{P_k\}=\{m_0, R_c, J_c, r\}$. The complete set of dimensionless groups related to the fluid flow is $\{\Pi\}=\{\mathrm{Re}, h/R_C, R_a/R_C, R_e/R_C\}$, where $\mathrm{Re} = r \hat{V}_{ZS} \hat{Z}_S / m$. Because R_a is the only element of $\{P\}$ that depends on the heat transfer in the arc, the dimensionless group R_a/R_C will be neglected in this isothermal formulation. The group R_e/R_C is also of little importance, because its influence is confined mainly to the cathode boundary layer, outside the cathode region. The variations generated by these groups are very small, suggesting that these are reasonable simplifications. The boundary conditions for the scaling of the fluid flow are represented in Table 2. Previous knowledge about the problem (from experiments and numerical models) indicate that the functions vary smoothly between the corner points.

Table 2
Boundary conditions for scaling of the fluid flow

	E	**F**	**G**	**H**
V_R	0	$\approx$-V_{RS}	$\approx$0	0
V_Z	$\approx$0	$\approx$0	$\approx$0	$\approx V_{ZS}$

The functions describing the fluid flow can be scaled with the following relationships:

$$R = R_C r \tag{13}$$

$$Z = Z_S z \tag{14}$$

$$V_R(R,Z) = V_{RS} r v_r(r,z) \tag{15}$$

$$V_Z(R,Z) = V_{ZS}\left[v_{z0}(z) - f_{VZ2}(\mathrm{Re}, h/R_C, R_a/R_C) r^2 v_z(r,z)\right] \tag{16}$$

$$P(R,Z) = P_S\, p(r,z) \tag{17}$$

The scaling of $V_Z(R, Z)$ is such that it varies in a quadratic manner in R at R=0, as eq. (1) to (3) indicate. The characteristic values Z_S, V_{RS}, V_{ZS}, and P_S can be estimated by balancing the equation of mass conservation eq. (1), the inertial, pressure and electromagnetic terms in the equation of conservation of momentum in R (2), and the inertial and pressure terms in the equation of conservation of momentum in Z (3). These estimations are compared with numerical results in Figure 2.

$$\hat{Z}_S = \tfrac{1}{2} R_C \tag{18}$$

$$\hat{V}_{RS} = \tfrac{1}{2} \frac{m_0^{\frac{1}{2}} R_C J_C}{r^{\frac{1}{2}}} \tag{19}$$

$$\hat{V}_{ZS} = \tfrac{1}{2} \frac{m_0^{\frac{1}{2}} R_C J_C}{r^{\frac{1}{2}}} \tag{20}$$

$$\hat{P}_S = \tfrac{1}{2} m_0 R_C^{\,2} J_C^{\,2} \tag{21}$$

The estimations of eq. (18) to (21) are valid when all of the terms in the normalized equivalent of the governing equations (eq. (1) to (6)) have a magnitude of one or less. This is true for $\mathrm{Re} > 1$, $R_a/R_C > 2$, and $h/R_C > \tfrac{1}{2}\Delta R^2/(R_a R_C)$. In order to avoid the effects of the anode on the cathode region, an additional condition is necessary: $h/Z_S >> 1$. These conditions are met for all of the cases considered in Table 3. The estimations of the characteristic parameters for the fluid flow can be corrected with expressions depending on the complete set of dimensionless groups. As was explained above, only two of these groups are significant, and the order of magnitude scaling methodology indicates that the corrections should be fairly smooth. Therefore the characteristic values can be approximated accurately by the following set of equations:

$$Z_S = \hat{Z}_S\, f_Z(\mathrm{Re}, h/R_C) \tag{22}$$

$$V_{RS} = \hat{V}_{RS}\, f_{VR}(\mathrm{Re}, h/R_C) \tag{23}$$

$$V_{ZS} = \hat{V}_{ZS}\, f_{VZ}(\mathrm{Re}, h/R_C) \tag{24}$$

$$P_S = \hat{P}_S\, f_P(\mathrm{Re}, h/R_C) \tag{25}$$

The correction functions are unknown, but with the help of the numerical calculations performed for this work and summarized in Table 3, an accurate expression of the form of a power law can be proposed:

$$f_Z = 0.88\,\mathrm{Re}^{0.058}\left(h/R_C\right)^{0.34} \tag{26}$$

$$f_{VR} = 0.22\,\mathrm{Re}^{-0.026}\left(h/R_C\right)^{0.086} \tag{27}$$

$$f_{VZ} = 0.55\,\mathrm{Re}^{0.073}\left(h/R_C\right)^{0.0068} \tag{28}$$

$$f_P = 0.13\,\mathrm{Re}^{0.17}\left(h/R_C\right)^{-0.057} \tag{29}$$

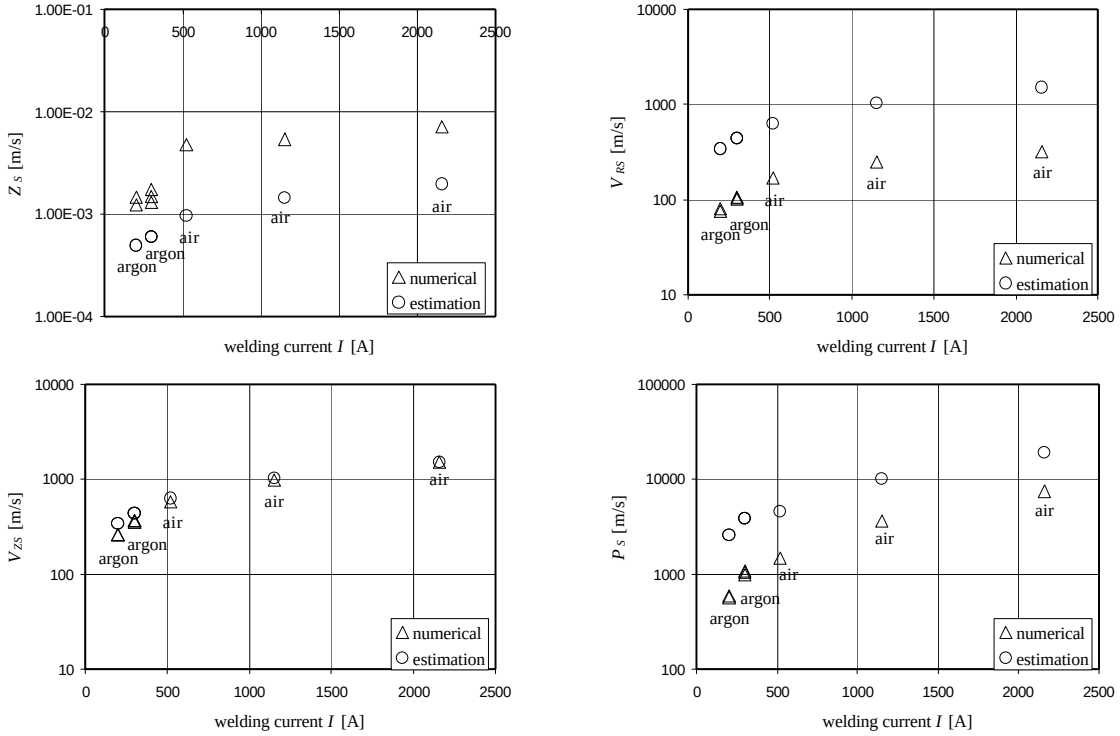

Figure 2

Estimations and numerical calculations of V_{RS}, V_{ZS}, P_S, and Z_S. In all cases the estimations predict the correct order of magnitude and functional dependence. The difference between numerical results and the estimations depend mainly on two dimensionless groups: Re, and h/R_C.

Discussion

The estimations obtained for maximum velocity and pressure have the same functional form as those previously proposed [3, 5, 6], although they were derived neither solving the differential equations, nor by imposing functional forms of the solutions, nor by assuming a priori which the dominant forces are. The goal of the estimations obtained here is to provide the correct functional dependence and the proper order of magnitude of the solutions; however eq. (P est) is exactly the same as obtained by Maecker, and eq. (VZ est) is a better approximation than Maeckert's equivalent expression (Maeckert's numerical coefficient overestimates the maximum velocity, while the coefficient obtained here generates estimations closer to the actual values). The previously existing approximate algebraic expressions can be improved with the use of a constant correction factor, as done by McKelliget *et al.* The drawback of that approach is that a constant factor is usually not enough, and its dependence is uncertain. The functions eq. (26) to (29) proposed here fulfill the role of a correction factor, but their functional dependence is clearly understood. The small exponents in their power law expression indicates that the estimations capture the essence of the behavior of the solution. The exponent of h/R_C in f_Z is significantly larger than all the other exponents suggesting that Z_S is especially sensitive to the arc length.

The hypothesis of laminar flow in the cathode region is justified by analyzing the onset of turbulence in an axisymmetric jet, which corresponds to a Reynolds number based on true velocity and of the order of 10^5 [8]. All of the cases analyzed here have true Reynolds numbers smaller that 3×10^3. If the fluid flow depended only on Re and

h/R_C, the exact solution could be expressed by eq. (22) to (25); however, the actual problem depends on many more parameters, some of them including thermal properties and their variations. The effect of the simplifications made to the scaling of this problem is translated into an error around the corrected values, and the magnitude of this error is an indication of the quality of the simplifications. For the cases of Table 3, the maximum error for f_Z is 13 %, for f_{VR} is 6 %, for f_{VZ} is 3 %, and for f_P is 8 %.

Table 3
Numerical results used to obtain the correction functions of eq. (26) to (29)

gas	electrode	I [A]	h [m]	T_{max} [K]	r [kg/m2]	m [kg/m s]	Z_S [m]	V_{RS} [m/s]	V_{ZS} [m/s]	P_S [Pa]
argon	W	200	0.01	21600	1.12E-02	5.41E-05	1.22E-03	76	256	574
argon	W	200	0.02	21500	1.12E-02	5.41E-05	1.47E-03	80	266	597
argon	W	300	0.0063	23200	9.97E-03	4.59E-05	1.30E-03	101	353	1084
argon	W	300	0.01	23200	9.97E-03	4.59E-05	1.49E-03	104	363	1062
argon	W	300	0.02	23100	9.97E-03	4.59E-05	1.75E-03	105	372	989
air	C	520	0.07	17200	5.70E-03	3.26E-05	4.76E-03	170	574	1492
air	C	1150	0.07	19500	4.71E-03	1.87E-05	5.43E-03	247	983	3653
air	C	2160	0.07	21300	4.23E-03	1.64E-05	7.09E-03	318	1498	7524

Conclusions

The estimations of the characteristic values obtained through the order of magnitude scaling technique (eq. (18) to (21)) are consistent with previous analytical expressions and are of the correct order of magnitude (Figure 2). The combination of these estimations with numerical calculations provides accurate predictions of the characteristic values (eq. (22) to (25) and eq. (26) to (29)). The small error between the corrected estimations and the numerical calculations suggests that no important mechanism was excluded in the simplifications. The small exponent of the correction functions also indicates that the estimations capture the essence of the behavior of the solutions. The dominant balance technique indicates that in the cathode region viscous effects are small, and the electromagnetic pressure created by the flow of the current through the plasma is balanced by the radial and axial inertial forces.

Notation

Upper-case symbols correspond to magnitudes with units, and lower case symbols correspond to their dimensionless counterparts. The subscripts *R*, and *Z* indicate radial and axial components of a vector, as indicated in Figure 1, the subscript *S* indicates that the magnitude in question is a characteristic parameter (or scaling factor). The hat ($\hat{}$)on top of a magnitude indicates that it is an estimation. The symbols *V*, *P*, *B*, and *J* represent velocity, pressure, magnetic field and current density in the cathode region. The greek symbols r, m, and m_0 represent density, viscosity of the plasma and the permeability of vacuum.

References

1. Mendez, P.F., (1999): Doctor of Philosophy, Massachusetts Institute of Technology.
2. Bender, C.M. and S.A. Orszag (1978): *Advanced Mathematical Methods for Scientists and Engineers*, McGraw-Hill.
3. Maecker, H. (1955): *Z. Phys.*, Vol. 141, pp. 198-216.
4. Burleigh, T.D., (1980): Master of Science, Massachusetts Institute of Technology.
5. Allum, C.J. (1981): *Journal of Physics D: Applied Physics*, Vol. 14, pp. 1041-1059.
6. McKelliget, J.W. and J. Szekely (1983): *Journal of Physics D: Applied Physics*, Vol. 16, pp. 1007-1022.
7. Hsu, K.C., K. Etemadi, and E. Pfender (1983): *Journal of Applied Physics*, Vol. 54, pp. 1293-1301.
8. McKelliget, J. and J. Szekely (1986): *Metallurgical Transactions A*, Vol. 17A, pp. 1139-1147.